# FoxM1 regulates re-annealing of endothelial adherens junctions through transcriptional control of β-catenin expression

Muhammad K. Mirza,[1] Ying Sun,[1] Yidan D. Zhao,[1] Hari-Hara S.K. Potula,[1] Randall S. Frey,[2] Steven M. Vogel,[1] Asrar B. Malik,[1] and You-Yang Zhao[1]

[1]Department of Pharmacology and Center for Lung and Vascular Biology, and [2]Department of Medicine, University of Illinois College of Medicine, Chicago, IL 60612



**Repair of the injured vascular intima requires a series of coordinated events that mediate both endothelial regeneration and reannealing of adherens junctions (AJs) to form a restrictive endothelial barrier. The forkhead transcription factor FoxM1 is essential for endothelial proliferation after vascular injury. However, little is known about mechanisms by which FoxM1 regulates endothelial barrier reannealing. Here, using a mouse model with endothelial cell (EC)-restricted disruption of *FoxM1* (*FoxM1 CKO*) and primary cultures of ECs with small interfering RNA (siRNA)-mediated knockdown of FoxM1, we demonstrate a novel requisite role of FoxM1 in mediating endothelial AJ barrier repair through the transcriptional control of β-catenin. In the *FoxM1 CKO* lung vasculature, we observed persistent microvessel leakage characterized by impaired reannealing of endothelial AJs after endothelial injury. We also showed that FoxM1 directly regulated β-catenin transcription and that reexpression of β-catenin rescued the defective AJ barrier–reannealing phenotype of FoxM1-deficient ECs. Knockdown of β-catenin mimicked the phenotype of defective barrier recovery seen in FoxM1-deficient ECs. These data demonstrate that FoxM1 is required for reannealing of endothelial AJs in order to form a restrictive endothelial barrier through transcriptional control of β-catenin expression. Therefore, means of activating FoxM1-mediated endothelial repair represent a new therapeutic strategy for the treatment of inflammatory vascular diseases associated with persistent vascular barrier leakiness such as acute lung injury.**

CORRESPONDENCE
You-Yang Zhao:
yyzhao@uic.edu

Abbreviations used: AJ, adherens junction; BW, body weight; ChIP, chromatin immunoprecipitation; EC, endothelial cell; HMVEC-L, human lung microvascular ECs; PAR-1, protease-activated receptor 1; siRNA, small interfering RNA; scRNA, scrambled control RNA; TER, transendothelial electrical resistance; VE-cadherin, vascular endothelial cadherin.

Maintenance of endothelial barrier function and establishing its set point in vascular inflammation plays a critical role in vascular homeostasis (Dejana, 2004; Aird, 2007; Lampugnani and Dejana, 2007). The endothelial monolayer controls the transvascular flux of fluid, proteins, and cells across the vessel wall into underlying tissues (Dejana et al., 2008). Although small increases in endothelial permeability such as those induced by vascular endothelial growth factor are beneficial to normal organs because they increase supply of nutrients and oxygen to tissues, severe loss of endothelial barrier function causes excessive build-up of fluid leading to organ dysfunction and chronic inflammation (Weis and Cheresh, 2005). In such cases, there is a persistent increase in endothelial permeability, hemorrhage, leukocyte transmigration, and formation of microthrombi (Mehta and Malik, 2006; Dejana et al., 2008). An uncontrolled increase in vascular permeability is the hallmark of a variety of inflammatory disorders including acute lung injury (Ware and Matthay, 2000; Mehta and Malik, 2006). In this context, it would be valuable to have novel approaches for the therapeutic control of vascular permeability based on the reannealing of the endothelial barrier.

Adherens junctions (AJs) play a crucial role in the regulation of endothelial barrier function (Bazzoni and Dejana, 2004; Mehta and Malik, 2006). AJs in the endothelium are composed of vascular endothelial cadherin



The Rockefeller University Press $30.00
J. Exp. Med. Vol. 207 No. 8 1675-1685
www.jem.org/cgi/doi/10.1084/jem.20091857

(VE-cadherin), α-catenin, β-catenin, and p120-catenin (Lampugnani et al., 1995; Aberle et al., 1996). Endothelial cells (ECs) forming a monolayer adhere to one another by a homotypic interaction between the extracellular domains of VE-cadherin. VE-cadherin binds β-catenin via its cytoplasmic domain, which in turn binds the actin-associated protein α-catenin. β-catenin, a member of *armadillo* repeat family of proteins, plays a particularly important role in AJ integrity (Cattelino et al., 2003). The interaction of VE-cadherin with β-catenin determines the stability of cell–cell junctions, and it is required for control of endothelial permeability (Cattelino et al., 2003). Intercellular adhesion between truncated VE-cadherin mutants that do not bind to β-catenin induced severely weakened AJs and resulted in fetal death in mice (Navarro et al., 1995; Carmeliet et al., 1999). The cytoplasmic domain of cadherins is also unstructured in the absence of β-catenin, and cadherin binding with β-catenin prevented the recognition of cadherins by degradation pathways (Huber et al., 2001). Thus, β-catenin, an integral component of the endothelial intercellular AJs, is required for normal endothelial barrier function.

Forkhead box M1 (FoxM1) is a member of the fox family of transcription factors that share homology in their winged helix DNA-binding domains (Clark et al., 1993; Kaestner et al., 2000). FoxM1 is a proliferation-associated transcription factor that controls both G1/S and G2/M phase progression by transcriptional regulation of a set of genes essential for cell cycle progression, including the cyclin-dependent kinase inhibitors $p21^{Cip1}$ and $p27^{Kip1}$, Cdc25A and Cdc25B, Aurora B kinase, and Polo-like kinase 1 (Kalinichenko et al., 2004; Costa, 2005; Laoukili et al., 2005; Wang et al., 2005; Wierstra and Alves, 2007). *FoxM1*-null mutation causes embryonic lethality in mice due to impaired execution of mitosis (Korver et al., 1998; Krupczak-Hollis et al., 2004). We have previously identified a critical role of FoxM1 in regulating endothelial regeneration after vascular injury (Zhao et al., 2006). Using mutant mice with EC-restricted disruption of FoxM1 (*FoxM1 CKO*), we observed that FoxM1 deficiency resulted in defective EC proliferation due to the sustained expression of $p27^{Kip1}$ and decreased expression of cyclins and Cdc25C after lung vascular injury induced by lipopolysaccharide. Thus, *FoxM1 CKO* mice exhibited severely impaired recovery of endothelial barrier function (Zhao et al., 2006). Given the fact that endothelial repair requires endothelial regeneration as well as reannealing of AJs to form the restrictive endothelial barrier, we addressed here whether FoxM1 mediates endothelial barrier repair by promoting AJ assembly. Thus, we determined the role of FoxM1 in mediating the expression of β-catenin and restoration of endothelial barrier function. Our results show that FoxM1 mediates AJ reannealing through the transcriptional control of β-catenin expression during endothelial repair.

## RESULTS

### Deletion of FoxM1 induces defective endothelial barrier recovery in vessels and endothelial monolayers after PAR-1 activation

To inactivate FoxM1 in the endothelium, mice carrying a *FoxM1* gene in which exons 4–7 were flanked by two *loxP* sites were bred with *Tie2* promoter/enhancer-driven *Cre* transgenic mice (Zhao et al., 2006). *Tie2* promoter/enhancer-driven Cre expression resulted in EC-restricted disruption of FoxM1 (Zhao et al., 2006). Activation of the protease-activated receptor 1 (PAR-1) by either PAR-1–specific activating peptide or thrombin induces endothelial barrier dysfunction through disruption of AJs (Coughlin, 2000; Vogel et al., 2000; Birukova et al., 2004; Broman et al., 2006; Camerer et al., 2006; Mehta and Malik, 2006). Using the isolated-perfused lung model (Vogel et al., 2000; Tiruppathi et al., 2002; Zhao et al., 2006), we observed that the basal lung capillary filtration coefficient ($K_{f,c}$), a measure of vascular permeability, of *FoxM1 CKO* mice was similar to WT. In response to PAR-1–specific peptide (TFLLRN-NH2), *FoxM1 CKO* lungs had the same increase in $K_{f,c}$ at 30 min after challenge as the WT. However, $K_{f,c}$ in *FoxM1 CKO* lungs remained significantly elevated for at least 4 h after challenge, whereas $K_{f,c}$ in WT returned to baseline within 2.5 h of PAR-1 activation (Fig. 1), which is indicative of impaired reannealing of the endothelial barrier in *FoxM1 CKO* lungs.

To gain insights into the mechanism of FoxM1 in regulating endothelial barrier function, we used small

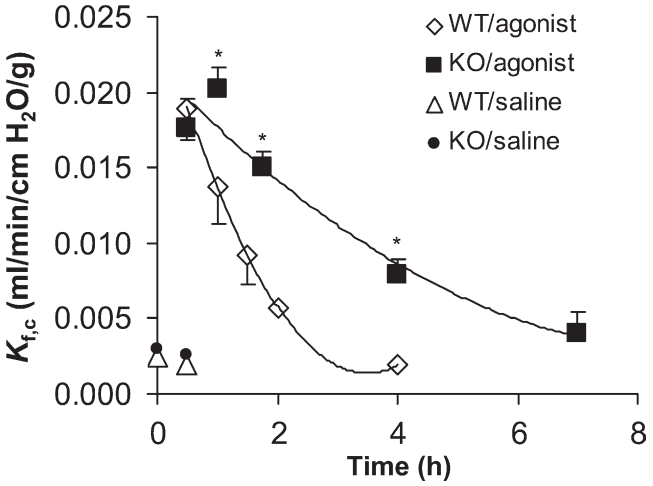


**Figure 1. Impaired reannealing of the endothelial barrier after an increase in lung vascular permeability induced by PAR-1 activation in *FoxM1 CKO* mice.** *FoxM1 CKO* mice or WT littermates were treated with either saline or a PAR-1 agonist peptide (i.v., 5 mg/kg BW). Lungs were isolated at the indicated times and perfused for $K_{f,c}$ measurements. $K_{f,c}$ was also measured at baseline (time 0). Data are expressed as mean ± SD (error bars; $n = 3$). *, $P < 0.05$ versus WT/agonist. Agonist, PAR-1 agonist peptide. Three independent experiments were performed with 20 WT and 21 *FoxM1 CKO* mice at the age of 3.5–4 mo old. *FoxM1 CKO* lungs exhibited persistent microvessel leakage after PAR-1 activation.

interfering RNA (siRNA) to knock down FoxM1 in endothelial monolayers, and measured transendothelial electrical resistance (TER) to quantify time-dependent changes in the integrity of endothelial AJs. After transfection with either FoxM1 siRNA or scrambled control RNA (scRNA; Kalinichenko et al., 2004), human lung microvascular ECs (HMVEC-L) were plated at confluent density on gold electrodes to form cell–cell contact and intact monolayers before induction of FoxM1 deficiency by siRNA. Mock transfection of HMVEC-L was also used as a control. At 65 h after transfection, the three groups of endothelial monolayers exhibited similar basal barrier function assessed by TER (Figs. 2 A and S1). Monolayers were then challenged with thrombin (4 U/ml), and changes in TER were monitored for 3 h. We observed similar decreases in TER in all groups in response to thrombin (Figs. 2 A and S1), which is indicative of similar AJ disruption. However, TER in FoxM1 siRNA-transfected cells failed to recover even at 10 h after the thrombin challenge, whereas scRNA and mock-transfected cells had fully recovered TER within 3 h (Figs. 2 A and S1). These findings were consistent with the data in the previous paragraph in the intact mouse lung vessels. We also observed defective recovery of endothelial barrier in FoxM1-deficient EC monolayers after challenge with histamine (Fig. S2), which indicates that the defective AJ barrier recovery response was not mediator specific. Using confocal microscopy, we observed that both control and FoxM1-deficient EC monolayers formed intact cell–cell junctions at baseline and exhibited similar AJ disruption at 20 min after the thrombin challenge (Fig. 3). scRNA-transfected HMVEC-L reformed an intact monolayer at 120 min after challenge, whereas the defect persisted up to 240 min after the thrombin challenge in siRNA-transfected HMVEC-L (Fig. 3).

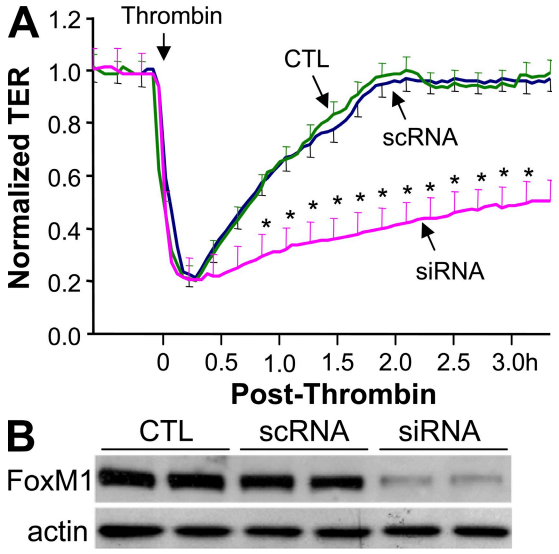


**Figure 2. Requirement of FoxM1 for reforming a restrictive barrier in ECs after PAR-1 activation.** (A) TER assay of endothelial AJ integrity in response to thrombin challenge (PAR-1 activation). HMVEC-L transfected with either human FoxM1 siRNA (siRNA) or scRNA, or mock-transfected (CTL), were plated to confluency on electrodes. AT 65 h after transfection, TER of each monolayer at baseline was recorded, and it was then monitored for 3 h after thrombin challenge (4 U/ml). TER values of each monolayer were normalized to their values at basal levels. Data are expressed as mean ± SD (error bars; $n = 3$ independent experiments). *, $P < 0.05$ versus either CTL or scRNA. FoxM1 deficiency induced a defective recovery of the endothelial barrier function after thrombin challenge. (B) Western blot analysis demonstrating siRNA-mediated knockdown of FoxM1 in HMVEC-L. At 65 h after transfection, HMVEC-L were lysed, and 15 µg of each lysate per lane was loaded for detection of FoxM1 protein level with anti-FoxM1 antibody. The same membrane was blotted with anti-actin antibody for loading control. The experiment was performed three times with similar results.

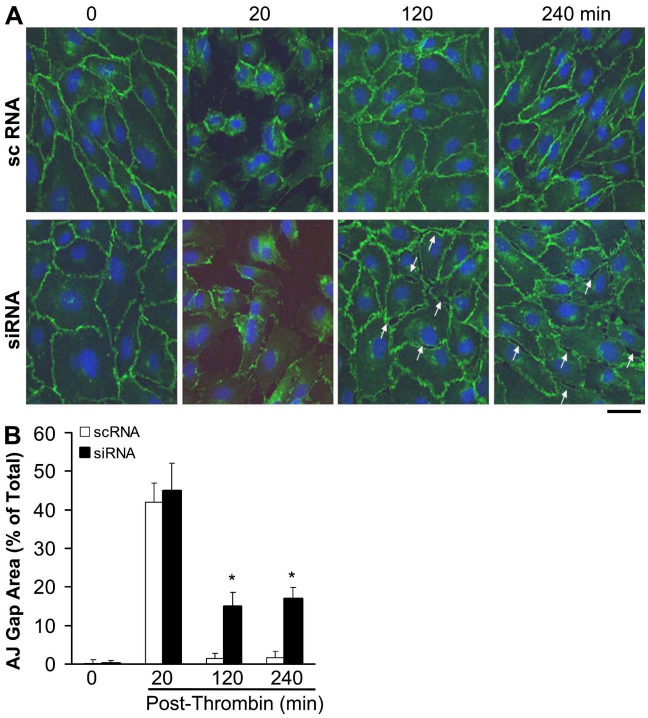


**Figure 3. Confocal microscopy of endothelial junctions after PAR-1 activation.** (A) Representative micrographs of anti–VE-cadherin staining. After transfection with either human FoxM1 siRNA (siRNA) or scRNA, HMVEC-L were plated in 24-well plates with a glass coverslip in each chamber at 100% confluency. At 65 h after transfection, the cells were treated with 4 U/ml thrombin in triplicate, and fixed with 4% paraformaldehyde at the indicated times. The fixed cells were immunostained with anti–VE-cadherin antibody (green) to visualize junctions, and nuclei were counterstained with DAPI (blue). FoxM1-deficient HMVEC-L (siRNA-transfected) exhibited defective reannealing of AJs at 2 and 4 h after thrombin challenge, in contrast to scRNA-transfected controls (scRNA). Arrows indicate failure of reannealing of AJs. The experiment was performed three times with similar data. Bar, 50 µm. (B) Quantification of intercellular AJ gap area. The area of intercellular AJ gaps was quantified using MetaMorph 7.1.0 by manually outlining cells and selecting for gaps. Values are expressed as the percentage of total surface area. Data are expressed as mean ± SD (error bars; $n = 3$ independent experiments). *, $P < 0.05$ versus scRNA at 120 and 240 min after thrombin challenge.

### FoxM1 deficiency induces decreased β-catenin expression in ECs

We performed quantitative RT-PCR analysis to assess expression of genes important for the formation of the endothelial AJ complex. As shown in Fig. 4 A, only β-catenin expression was decreased among the AJ components. Western blot analysis demonstrated markedly decreased basal β-catenin protein expression in FoxM1-deficient HMVEC-L as well as after the thrombin challenge, whereas protein levels of other AJ components—VE-cadherin, α-catenin, and p120-catenin—were unchanged (Fig. 4, B and C). As shown in Fig. 4 (D and E), β-catenin expression in the membrane fraction was markedly decreased basally in confluent FoxM1-deficient HMVEC-L, whereas the cytosolic β-catenin fraction did not change. After the thrombin challenge, β-catenin membrane expression was decreased in both scRNA- and siRNA-treated cells at 20 min, and its cytosolic expression was increased. β-catenin membrane and cytosolic expression returned to basal levels at 2 h after the thrombin challenge in scRNA-treated HMVEC-L, but not in the FoxM1-deficient cells (Fig. 4, D and E).

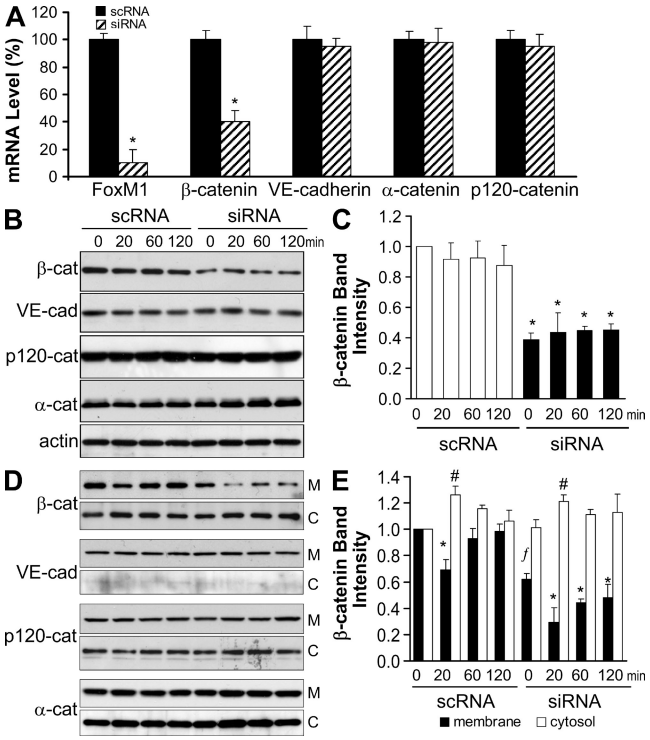


**Figure 4. Decreased expression of β-catenin in FoxM1-deficient ECs.** (A) Quantitative RT-PCR analysis of expression of components of endothelial AJs. At 65 h after transfection of either FoxM1 siRNA or scRNA, confluent HMVEC-L were lysed for RNA isolation. mRNA levels of the indicated genes were quantified by quantitative RT-PCR analysis. Data are expressed as mean ± SD (error bars; $n = 3$). *, $P < 0.05$ versus scRNA. The experiment was performed three times with similar results.
(B and C) Western blot analysis demonstrating decreased protein levels of β-catenin in FoxM1-deficient HMVEC-L. At 65 h after transfection with either human FoxM1 siRNA (siRNA) or scRNA, confluent HMVEC-L were lysed for Western blot analysis of each protein. Anti-actin was used as a loading control (B). The experiment was performed three times with similar results. β-catenin expression was quantified by densitometry analysis (C). Data are expressed as mean ± SD (error bars; $n = 3$ independent experiments). *, $P < 0.05$ versus scRNA. (D and E) Subcellular localization of endothelial AJ proteins at baseline and after thrombin challenge. At 65 h after transfection, confluent HMVEC-L monolayers were collected for cell fractionation. Each membrane (M) or cytosolic (C) fraction (7.5 μg per lane) was loaded for detection of each protein (D). The experiment was performed three times with similar results. β-catenin localization in the membrane fraction versus cytosolic fraction was quantified by densitometry (E). Data are expressed as mean ± SD (error bars; $n = 3$ independent experiments). *, $P < 0.01$ versus membrane expression at time 0 (basal); #, $P < 0.05$ versus cytosolic expression at time 0; *f*, $P < 0.05$ versus scRNA-membrane expression at time 0.

### Decreased β-catenin expression is responsible for defective AJ reannealing

To address the role of decreased expression of β-catenin in mediating defective reannealing of AJs in FoxM1-deficient EC monolayers, plasmid DNA expressing β-catenin was transfected into HMVEC-L along with FoxM1 siRNA, and TER was measured to monitor the endothelial integrity. Re-expression of β-catenin in FoxM1-deficient HMVEC-L promoted recovery of AJ function after the thrombin challenge, in contrast to FoxM1-deficient HMVEC-L monolayers transfected only with siRNA (Fig. 5, A and B).

To establish the level of β-catenin expression required for AJ recovery, we transfected various doses of plasmid DNA expressing β-catenin into FoxM1 siRNA-transfected HMVEC-L. As shown in Fig. 5 (C and D), reexpression of β-catenin in FoxM1-deficient HMVEC-L resulted in concentration-dependent AJ barrier recovery. Western blot analysis confirmed the increases in β-catenin expression (Fig. 5 E). Confocal microscopy showed restored membrane accumulation of β-catenin in confluent FoxM1-deficient HMVEC-L monolayers transfected with plasmid DNA (Fig. 6, A and B). Western blotting confirmed the increased expression of β-catenin in the membrane fraction with little change in the cytosolic fraction (Fig. 6 C). In confluent EC monolayers, β-catenin was predominantly localized at the membrane, as shown in Fig. 6 C (the enhanced band intensity of β-catenin expression in the cytosolic fraction shown in Fig. 4 D is caused by the prolonged exposure of the signal).

To determine whether the 50% reduction in β-catenin expression seen in FoxM1-deficient EC monolayers is sufficient to impair AJ reannealing, HMVEC-L were transfected with 1.5 μmol/L of β-catenin siRNA to achieve an ~50% reduction in β-catenin protein expression (Fig. 7, A and B). After transfection with either 1.5 μmol/L β-catenin siRNA or scRNA, HMVEC-L were plated at confluent density on gold electrodes to measure TER. These monolayers exhibited similar basal AJ barrier function at 48 h after transfection (Fig. 7 C). Upon challenge of monolayers with 4 U/ml thrombin, the resultant changes in TER were monitored for 6 h. We observed similar decreases of TER in β-catenin

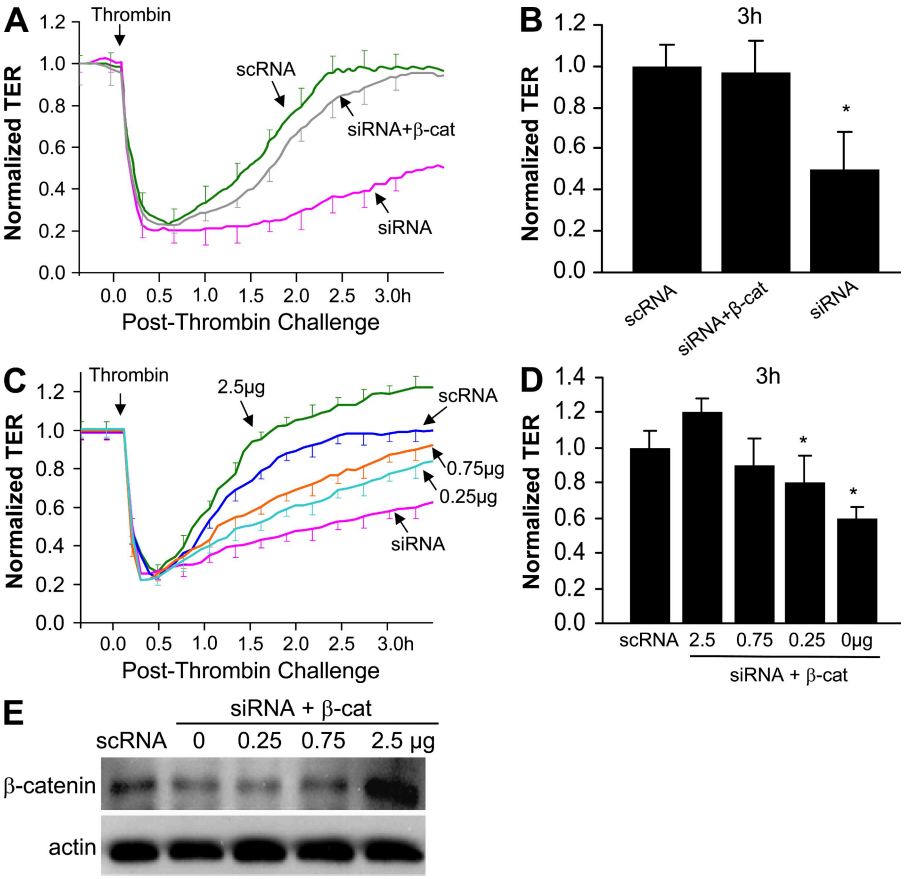


**Figure 5. Rescue of defective reannealing of endothelial AJ barrier of FoxM1-deficient ECs by restoration of β-catenin protein.** (A and B) Decreased β-catenin expression is responsible for impaired reannealing of the endothelial AJ barrier in FoxM1-deficient HMVEC-L. HMVEC-L were transfected with human FoxM1 scRNA, siRNA, and siRNA plus plasmid DNA expressing human β-catenin (siRNA+β-cat). At 65 h after transfection, the monolayers were challenged with 4 U/ml thrombin, and TER was recorded for 3 h. Data are expressed as mean ± SD (error bars; $n = 3$ independent experiments). *, $P < 0.05$ versus scRNA. (C and D) β-catenin expression rescued defective reannealing of the endothelial AJ barrier of FoxM1-deficient HMVEC-L in a dose-dependent manner. HMVEC-L were transfected with either FoxM1 scRNA, siRNA, or siRNA plus plasmid DNA expressing human β-catenin at the indicated amounts. At 65 h after transfection, monolayers were challenged with 4 U/ml thrombin, and TER was recorded for 3 h. Data are expressed as mean ± SD (error bars; $n = 3$ independent experiments). *, $P < 0.05$ versus scRNA. (E) Western blots demonstrating increased β-catenin expression in FoxM1-deficient HMVEC-L by plasmid DNA transfection. The experiment was performed three times with similar results.

siRNA-transfected cells compared with scRNA-transfected cells. However, β-catenin siRNA-transfected cells failed to regain baseline values, whereas scRNA-transfected monolayers recovered within 3 h of the thrombin challenge (Fig. 7 C). Collectively, these data demonstrate the causal role of β-catenin reduction in FoxM1-deficient EC monolayers in the mechanism of defective AJ barrier reannealing.

### β-catenin is a transcriptional target of FoxM1

FoxM1 regulates transcription of a set of genes essential for cell cycle progression (Kalinichenko et al., 2004; Costa, 2005; Laoukili et al., 2005; Wang et al., 2005; Wierstra and Alves, 2007). FoxM1 binding to the consensus site (TTTGTTT-GTTTT) activates transcription of these genes. We identified two potential FoxM1-binding sites in the 6-kb promoter region of the human *ctnnb1* gene (Fig. 8 A). To determine whether FoxM1 binding activates transcription of the *ctnnb1* gene, we used a chromatin immunoprecipitation (ChIP) assay. The cross-linked and sonicated chromatin from FoxM1 siRNA-transfected HMVEC-L was immunoprecipitated with either anti-FoxM1 or control IgG antibodies. Chromatin from either scRNA- or mock-transfected HMVEC-L was used as a control. FoxM1-bound β-catenin promoter DNA associated with immunoprecipitated chromatin was quantified by quantitative real-time PCR analysis with primers specific for the potential FoxM1 binding sites. As shown in Fig. 8 B, siRNA-mediated knockdown of FoxM1 resulted in a marked decrease in FoxM1-binding to promoter regions of the human *ctnnb1* gene.

To determine whether FoxM1-binding sites are transcriptionally active, a luciferase reporter assay was performed with constructs driven by a human *ctnnb1* promoter containing various deletions. As shown in Fig. 8 C, constructs a and b containing FoxM1-binding sites drove greater luciferase activity in subconfluent cells compared with confluent cells, which is consistent with the protein levels of FoxM1 in these conditions (Fig. 8 D). A construct with deletion of the two FoxM1-binding sites (construct c) abolished transcription activity in both confluent and subconfluent conditions. These data demonstrate that β-catenin as a transcriptional target of FoxM1.

### Restoration of β-catenin expression in *FoxM1 CKO* lungs rescues the defective endothelial AJ reannealing phenotype

To determine whether genetic deletion of FoxM1 in EC monolayers induces decreased β-catenin expression, lung microvascular ECs and fibroblasts (used for comparison purpose) were isolated from WT and *FoxM1 CKO* lungs, respectively. As shown in Fig. 9 A, FoxM1 deficiency in EC sdown-regulated β-catenin expression only in ECs. The protein level of β-catenin was reduced ~30% in *FoxM1 CKO* lungs compared with WT (Fig. 9 B). Interestingly, increased expression of γ-catenin (plakoglobin) and catenin-d2 was observed in FoxM1-deficient ECs (Fig. 9 A). We next

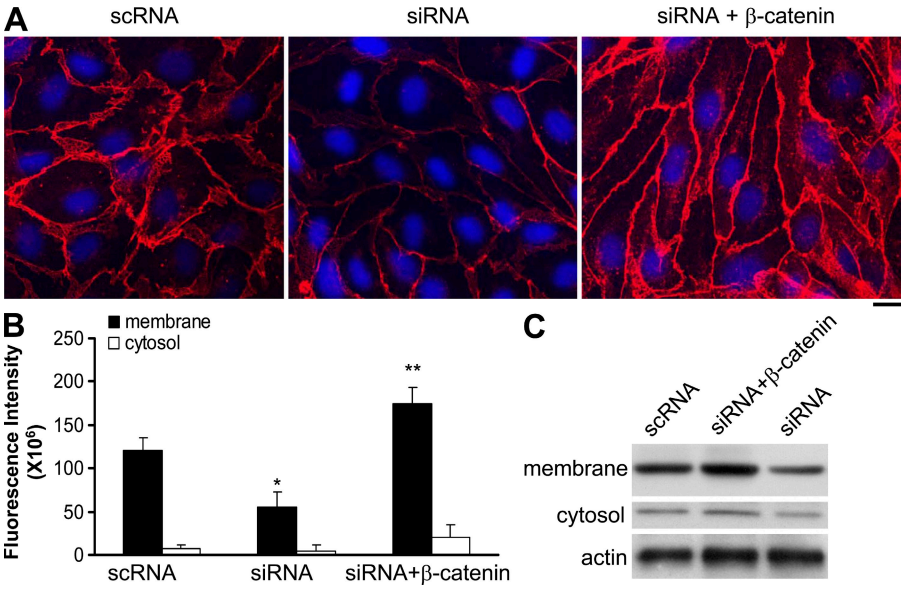


**Figure 6. Decreased membrane expression of β-catenin in confluent FoxM1-deficient ECs.** (A) Representative micrographs of immunofluorescent staining with anti–β-catenin antibody. At 65 h after transfection with either human FoxM1 scRNA, siRNA, or siRNA plus plasmid DNA expressing human β-catenin (siRNA+β-catenin, 1.5 μg/$10^6$ cells), monolayers were fixed and immunostained with anti–β-catenin antibody to visualize β-catenin (red). Nuclei were counterstained with DAPI (blue). The experiment was performed three times with similar results. Bar, 20 μm. (B) Quantification of fluorescent intensity demonstrating reduced membrane expression of β-catenin in FoxM1-deficient HMVEC-L, which was restored by exogenous β-catenin expression. Accumulation of β-catenin at the membrane was quantified using 12-bit depth confocal z-series images. Maximum pixel values from different z sections were projected to a single plane using MetaMorph 7.1.0. Integrated fluorescence intensity of threshold projected images was calculated for β-catenin. Data are expressed as mean ± SD (error bars; $n = 3$ independent experiments). *, $P < 0.05$ versus scRNA. **, $P < 0.01$ versus siRNA. (C) Western blot analysis demonstrating decreased β-catenin protein levels in the membrane fraction in confluent FoxM1-deficient HMVEC-L. At 65 h after transfection, confluent HMVEC-L monolayers were collected for cell fractionation. Each membrane fraction or cytosolic fraction (7.5 μg per lane) was loaded for detection of β-catenin with anti–β-catenin antibody. The experiment was performed three times with similar results.

addressed whether restoration of the β-catenin protein level in *FoxM1 CKO* lungs would result in the normalization of AJ reannealing. As shown in Fig. 9 B, liposome-mediated transduction of plasmid DNA expressing β-catenin restored the protein expression of β-catenin in *FoxM1 CKO* mouse lungs. At 40 h after transduction, these mice were challenged with a PAR-1 agonist peptide (i.v., 5 mg/kg body weight [BW]). Lungs were isolated at 2 h after challenge and perfused for $K_{f,c}$ measurements. In contrast to the $K_{f,c}$ value in control *FoxM1 CKO* lungs, restoration of β-catenin protein expression in *FoxM1 CKO* lungs resulted in a $K_{f,c}$ value similar to WT lungs (Fig. 9 C); thus, AJ reannealing of endothelial barrier in *FoxM1 CKO* lungs was restored by β-catenin expression.

## DISCUSSION

We have identified here the novel role of the transcription factor FoxM1 in regulating the reannealing of endothelial AJs through the transcriptional control of β-catenin expression. *FoxM1 CKO* lungs exhibited defective reannealing of endothelial barrier phenotype after AJ disruption induced by PAR-1 activation. FoxM1 deficiency in EC monolayers impaired AJ reannealing after activation of PAR-1 signaling. β-catenin expression was markedly decreased in FoxM1-deficient EC monolayers, whereas reexpression of β-catenin rescued the defective AJ reannealing phenotype in both EC monolayers and *FoxM1 CKO* lung vessels. Knockdown of β-catenin mimicked the phenotype of defective barrier recovery seen in FoxM1-deficient ECs. We also show that FoxM1 specifically binds to the promoter regions of the human *ctnnb1* gene and control its transcription. Thus, β-catenin is a transcriptional target of FoxM1 whereby FoxM1 regulates formation of endothelial AJ assembly.

Endothelial repair after vascular injury is a crucial process required for vascular homeostasis in inflammatory disorders. Endothelial barrier repair involves endothelial regeneration through FoxM1 activation of cell proliferation (Zhao et al., 2006). As the present results show, the repair also involves FoxM1-induced activation of β-catenin transcription, which results in the reannealing of AJs to form the characteristic restrictive endothelial barrier. Our previous study demonstrated the critical role of FoxM1 in regulating endothelial regeneration after lung vascular injury (Zhao et al., 2006). We showed that mice with EC-restricted disruption of FoxM1 exhibited long-lived increase of lung microvessel permeability and lung edema formation after LPS challenge. FoxM1 deficiency severely impaired endothelial proliferation in *FoxM1 CKO* lungs (Zhao et al., 2006). However, it was not clear whether FoxM1 can also regulate the actual reannealing of AJs to form the endothelial barrier. To address the process of AJ reannealing, we used the model of PAR-1 activation, which is known to disassemble AJs within 30 min (Birukova et al., 2004; Broman et al., 2006; Zhao et al., 2010) and increase the permeability of vessels (Coughlin, 2000; Vogel et al., 2000; Mehta and Malik, 2006, Camerer et al., 2006; Tauseef et al., 2008). We observed that *FoxM1 CKO* lung microvessels exhibited sustained leakage as determined by $K_{f,c}$ increases after PAR-1 activation, whereas either microvessel permeability at baseline or a maximal increase in permeability in response to PAR-1 activation was similar in *FoxM1 CKO* and WT lungs.

In primary culture of HMVEC-L, FoxM1 deficiency induced by siRNA also prevented the reannealing of AJs. These data collectively demonstrate the important role of FoxM1 in regulating reannealing of endothelial junctions after AJ disruption.

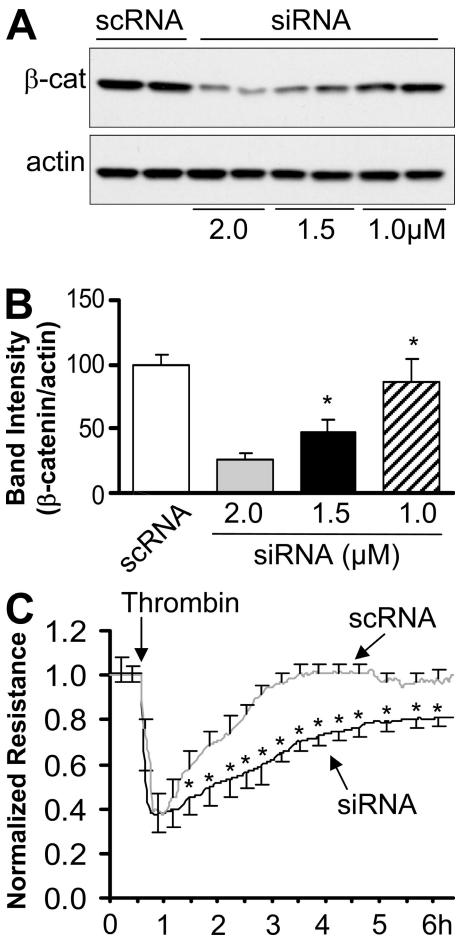


**Figure 7. Knockdown of β-catenin mimics the defective reannealing phenotype of endothelial junctions seen in FoxM1-deficient monolayers after PAR-1 activation.** (A and B) siRNA dose response of knockdown of β-catenin. At 48 h after transfection with β-catenin scRNA, or siRNA at indicated doses, the confluent HMVEC-L were lysed for Western blot analysis of β-catenin protein levels. The same membrane was blotted with anti-actin for loading control (A). The experiment was performed three times with similar results. Densitometry was used to quantify the protein levels of β-catenin under each condition (B). Data are expressed as mean ± SD (error bars; $n = 3$ independent experiments). *, $P < 0.05$ versus scRNA. 1.5 μmol/L of β-catenin siRNA induces ∼50% knockdown of β-catenin protein level. (C) TER assay demonstrating that partial knockdown of β-catenin results in impaired recovery of endothelial AJ function after thrombin challenge. HMVEC-L transfected with either human β-catenin siRNA (siRNA, 1.5 μmol/L) or scRNA were plated on electrodes at confluency. At 48 h after transfection, TER of each monolayer at baseline was recorded and monitored for 6 h after the thrombin challenge (4 U/ml). The TER value of each monolayer was normalized to its value at baseline. Data are expressed as mean ± SD (error bars; $n = 3$ independent experiments). *, $P < 0.05$ versus scRNA.

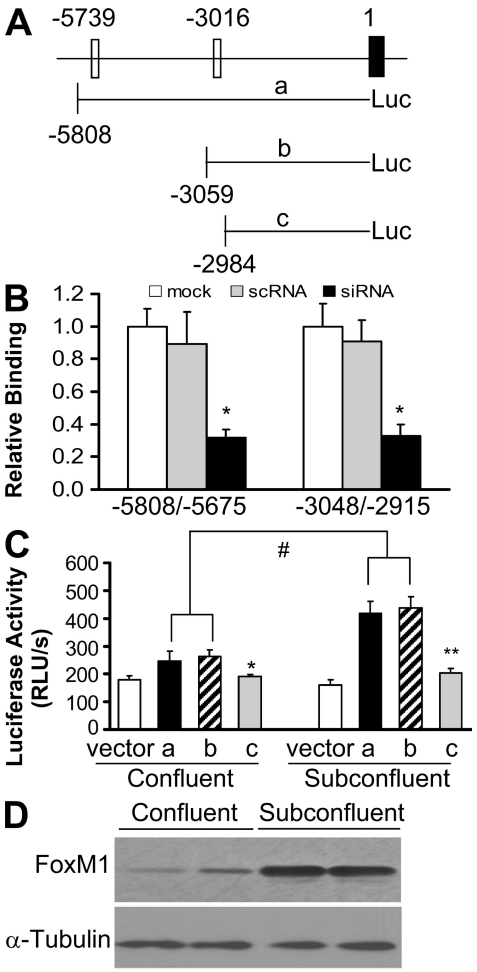


**Figure 8. FoxM1 regulation of β-catenin transcription.** (A) Schematic drawing of the 6-kb promoter region of the human *ctnnb1* gene. FoxM1 binding sites are indicated (open box); the first exon is also show (shaded box). The three luciferase reporter constructs with various deletions of FoxM1 binding sites are also shown. (B) ChIP assay demonstrating that FoxM1 directly binds to two promoter regions of the *ctnnb1* gene. Cross-linked chromatin from either mock-transfected or FoxM1 siRNA- or scRNA-transfected HMVEC-L was immunoprecipitated with either anti-FoxM1 antibody or IgG control. After immunoprecipitation, genomic DNA was analyzed for the amount of *ctnnb1* promoter DNA using quantitative real-time PCR with primers specific for each region. FoxM1 binding to genomic DNA was normalized to IgG control. Data are shown as mean ± SD (error bars; $n = 3$ independent experiments). *, $P < 0.05$ versus either mock or scRNA. (C) Luciferase reporter assay demonstrating that FoxM1 induced the transcriptional activity of the human *ctnnb1* gene. After transfection with either luciferase reporter constructs under the control of a promoter of the human *ctnnb1* gene with indicated deletions (a, b, and c) or empty vector (vector), HMVEC-L were plated at subconfluent (40%) or confluent conditions. At 40 h after transfection, the cells were collected for analysis of luciferase activity. Data are expressed as mean ± SD (error bars; $n = 3$ independent experiments). *, $P < 0.05$ versus either construct a or b at a confluent condition; #, $P < 0.01$ confluent versus subconfluent conditions; **, $P < 0.005$ versus either construct a or b at a subconfluent condition. (D) Western blot analysis demonstrating markedly decreased FoxM1 expression in confluent HMVEC-L. Cell lysates of HMVEC-L at 100% confluency and 50–70% confluency were used for Western blotting of FoxM1 expression. The experiment was performed three times with similar results.

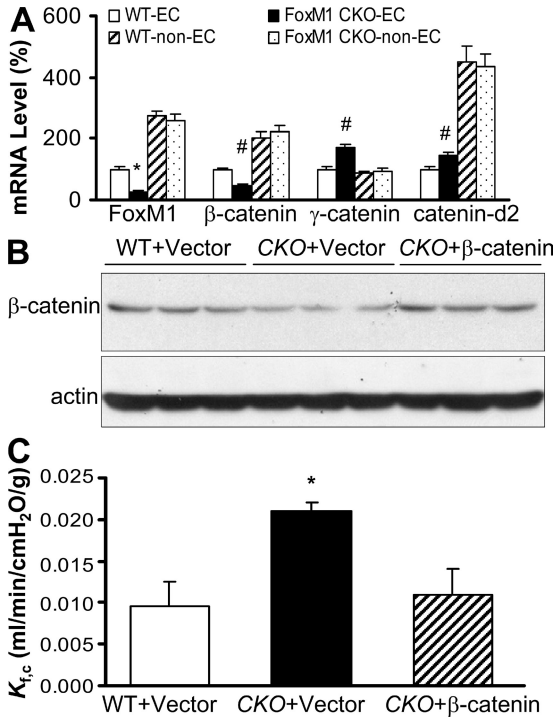


**Figure 9. Normalization of the endothelial AJ barrier by restoration of β-catenin expression after increased vascular permeability in *FoxM1 CKO* lungs.** (A) Quantitative RT-PCR analysis of gene expression. After 2 d in culture, microvascular ECs isolated from WT or *FoxM1 CKO* mouse lungs were lysed for total RNA isolation. Non-EC cultures (fibroblasts) were also lysed for total RNA isolation. mRNA levels of the indicated genes were quantified by quantitative RT-PCR. Data are expressed as mean ± SD (error bars; $n = 3$ independent experiments). *, $P < 0.01$ versus WT-EC; #, $P < 0.05$ versus WT-EC. (B) Western blotting demonstrating decreased β-catenin expression in *FoxM1 CKO* lungs compared with WT lungs and restoration of β-catenin expression by liposome-mediated transduction of plasmid DNA expressing β-catenin. The experiment was performed three times with similar results. *CKO*, *FoxM1 CKO*. (C) Normalization of vascular junctional repair by restoration of β-catenin expression in *FoxM1 CKO* lungs. Plasmid DNA expressing β-catenin or empty vector were transduced in *FoxM1 CKO* lungs through i.v. injection of the liposome–DNA complex. WT mice transduced with empty vector DNA were used as controls. At 40 h after transduction, mice were challenged with a PAR-1 agonist peptide (i.v., 5 mg/kg BW). Lungs were isolated at 2 h after challenge and perfused for $K_{f,c}$ measurement. Data are expressed as mean ± SD (error bars; $n = 3$–4 animals/group from three independent experiments). *, $P < 0.05$ versus either WT + vector, or *CKO* + β-catenin.

We observed a marked decrease in plasma membrane expression of β-catenin in FoxM1-deficient EC monolayers, whereas expression of other components of AJs (VE-cadherin, α-catenin, and p120-catenin) was not significantly affected. Importantly, expression of β-catenin in FoxM1-deficient EC monolayers rescued the defective AJ reannealing phenotype after PAR-1 activation. A 50% reduction of β-catenin in EC monolayers induced by siRNA mimicked the phenotype of defective AJ reannealing seen in FoxM1-deficient ECs, in which there was also a ∼50% reduction in β-catenin expression. These observations support the identified role of β-catenin in mediating the integrity of the endothelial AJ barrier (Navarro et al., 1995; Carmeliet et al., 1999; Huber et al., 2001; Cattelino et al., 2003).

FoxM1 regulates transcription of a set of genes required for cell cycle progression (Kalinichenko et al., 2004; Costa, 2005; Laoukili et al., 2005; Wang et al., 2005; Wierstra and Alves, 2007). Our results show that FoxM1 also regulates the transcription of β-catenin required for the integrity of endothelial AJs. FoxM1 binding to the *ctnnb1* promoter activated the transcription of β-catenin. We showed that the decreased β-catenin expression in FoxM1-deficient EC monolayers was the result of a loss of FoxM1-mediated transcription. These data identify a novel mechanism of repair of endothelial AJs through FoxM1-mediated transcription of β-catenin–mediating reannealing of endothelial AJs and endothelial barrier repair.

Given that FoxM1 was shown to regulate the transcription of the β-catenin gene and endothelial AJ barrier function, it would be expected that *FoxM1 CKO* vessels should have increased basal vascular permeability values. However, we observed that these values were normal in *FoxM1 CKO* lungs. This apparent discrepancy can be ascribed to genetic compensation, perhaps on the basis of expression of other AJ protein constituents. We observed increased expression of γ-catenin and catenin-d2 in FoxM1-deficient ECs isolated from *FoxM1 CKO* lungs, which may maintain basal permeability at a relatively normal set point despite the reduction in β-catenin expression in FoxM1-deficient ECs. It has been shown that γ-catenin can take over the role of β-catenin in cell adhesion and preserve intact AJs in β-catenin–deficient embryos (Huelsken et al., 2000). Another possible explanation is that the remaining pool of β-catenin protein is sufficient to seal the endothelial barrier. However, in the acute response to PAR-1 activation, any defects in β-catenin expression may be sufficient to impair reannealing of the endothelial barrier. Our studies provide unequivocal evidence that FoxM1-regulated β-catenin expression plays a crucial role in regulating the reannealing of endothelial AJs to reform the characteristic restrictive endothelial barrier after vascular injury.

In conclusion, the rapid restoration of the restrictive endothelial barrier is critical for vascular homeostasis, and the lack of full recovery of AJ barrier function can lead to chronic inflammation. This study shows the obligatory role of FoxM1 in regulating the reannealing of endothelial AJs through transcriptional control of β-catenin expression. We have demonstrated that FoxM1 regulates endothelial repair by not only inducing endothelial regeneration as shown (Zhao et al., 2006) but also in a more rapid manner by reforming and resealing the AJ endothelial barrier through expression of β-catenin. Thus, promotion of FoxM1-mediated endothelial regeneration and reannealing of endothelial AJs may represent a novel means of endothelial repair and restoring vascular homeostasis, and thereby preventing inflammatory diseases associated with persistently leaky vessels such as acute lung injury.

## MATERIALS AND METHODS

**Mice.** The generation of mice with EC-specific inactivation of *FoxM1* (*FoxM1 CKO*) has been described previously (Zhao et al., 2006). Littermates of genotypes of $FoxM1^{fl/fl}$ from the same breeding pair were used as WT, whereas $FoxM1^{fl/fl}$ and *Cre* were used as *FoxM1 CKO*. All mice were bred and maintained in the Association for Assessment and Accreditation of Laboratory Animal Care–accredited animal facilities at the University of Illinois at Chicago according to National Institutes of Health guidelines. All animal experiments were performed in accordance with protocols approved by the University of Illinois at Chicago Animal Care and Use Committee.

**Pulmonary microvascular permeability.** Microvessel $K_{f,c}$ was measured to determine the pulmonary microvascular permeability to liquids, as described previously (Vogel et al., 2000; Tiruppathi et al., 2002). In brief, after standard 30-min equilibration perfusion, the outflow pressure was rapidly elevated by 13 cm $H_2O$ for 20 min and then returned to normal. The changes of lung wet weight reflect net fluid extravasation. At the end of each experiment, lungs were dissected free of nonpulmonary tissue, and lung dry weight was determined. $K_{f,c}$ (ml/min/cm$H_2O$/dry weight [g]) was calculated from the slope of the recorded weight change normalized to the pressure change and to lung dry weight. PAR-1 agonist peptide (TFLLRN-NH2; Vogel et al., 2000; Tauseef et al., 2008) was administered via jugular vein injection, and lungs were isolated at various times for $K_{f,c}$ measurement.

**Primary cultures of lung microvascular ECs.** Primary cultures of HMVEC-L (Lonza) were cultured in T75 flasks precoated with 0.2% gelatin in EBM-2 complete medium supplemented with 15% FBS and EGM-2 MV Singlequots (Lonza), and maintained at 37°C in a humidified atmosphere of 5% $CO_2$ and 95% air. The cells were used for experiments between four and seven passages. To express β-catenin in HMVEC-L, human cDNA of β-catenin was cloned into expression vector pcDNA3.1 (provided by E.R. Fearon, University of Michigan Medical School, Ann Arbor, MI) and transfected into HMVEC-L using the HMVEC-L Nucleofector kit with the Amaxa Nucleofector device (Lonza).

Primary cultures of mouse lung microvascular ECs were established using cells immuno-selected from mouse lungs as described previously (Zhao et al., 2006). In brief, a cell suspension was prepared from lungs by digestion with 1 mg/ml collagenase and 0.5 mg/ml dispase for 30 min twice, followed by filtration using 70-µm and 40-µm nylon filters. ECs were then selected using a rat antibody to mouse CD-31 (Millipore) and a secondary antibody coupled to magnetic beads (Miltenyi Biotec). Purified ECs were plated on a 0.2% gelatin-coated T25 flask followed by a medium change on the second day. ECs were lysed for total RNA isolation after growing 2 d in EBM-2 complete medium (Lonza). Primary cultures of fibroblasts were established by collecting cells from the EC-depleted flow-through of the magnetic column and plating directly on T75 flask in DMEM made with 10% FBS (Invitrogen). Confluent cultures of these non-ECs were then trypsinized and replated. After four passages, these primary cultures of fibroblast-enriched non-ECs were used for experiments as controls.

**siRNA-mediated gene knockdown.** Both FoxM1 siRNA and scRNA were synthesized (Integrated DNA Technology) based on previously published sequences (Wang et al., 2005). The human β-catenin siRNA sequences are as follows: 5′-GUAGCUGAUAUUGAUGGACTT-3′ and 5′-GUCCAUCAAUAUCAGCUACTT-3′. The following human β-catenin scRNA sequences were used for controls: 5′-GUAUUGGCUGAUAAUACGGTT-3′ and 5′-CCGUAUUAUCAGCCAAUAC-3′. Transfection of either siRNA or scRNA was performed using the HMVEC-L Nucleofector kit (Lonza) according to the manufacturer's instructions. In brief, HMVEC-L cells grown to 90% confluence were trypsinized, pelleted, and resuspended in 100 µl of HMVEC-L nucleofector solution with 4 µl (2, 3, and 4 µl for β-catenin knockdown) of 50 µmol/L siRNA or scRNA. Cells were rapidly electroporated with an Amaxa Nucleofector device (Lonza), and then plated in EBM-2 complete medium for experiments.

**Molecular analysis.** Total RNA was isolated using an RNeasy Mini kit including DNase I digestion (Qiagen), and one-step quantitative RT-PCR analysis was performed with a sequence detection system (ABI Prism 7000; Applied Biosystems) with a QuantiTect SYBR Green PCR kit (QIAGEN). The following primers were used for analyses: human FoxM1 primers, 5′-GGAGGAAATGCCACACTTAGCG-3′ and 5′-TAGGACTTCTTGGGTCTTGGGGTG-3′; human β-catenin primers, 5′-CAAGTGGGTGGTATAGAGG-3′ and 5′-TCAATGGGAGAATAAAGCAGC-3′; human VE-cadherin primers, 5′-TCGCTGTTGTCACATCTCAGGGAA-3′ and 5′-TGACTGATGCCACTTCTCCAAGGT-3′; human 18S ribosomal RNA (rRNA), 5′-TTCCGACCATAAACGATGCCGA-3′and 5′-GACTTTGGTTTCCCGGAAGCTG-3′; mouse FoxM1 primers, 5′-CACTTGGATTGAGGACCACTT-3′ and 5′-GTCGTTTCTGCTGTGATTCC-3′; and mouse cyclophilin primers, 5′-CTTGTCCATGGCAAATGCTG-3′ and 5′-TGATCTTCTTGCTGGTCTTGC-3′. Primers for human p120-catenin and α-catenin, and for mouse β-catenin, γ-catenin, and catenin-d2 were obtained from QIAGEN. All human gene expression was normalized to human 18S rRNA as an internal control, whereas mouse FoxM1 expression was normalized to mouse cyclophilin as an internal control.

Western blot analyses were performed using antibodies against β-catenin (1:200), VE-cadherin (1:1,000), α-catenin (1:200), p120-catenin (1:200), and FoxM1 (1:1,000), respectively. All antibodies were purchased from Santa Cruz Biotechnology, Inc. The same blot was reprobed with anti-actin mAb (1:3,500; BD) for loading control.

**Transendothelial monolayer electrical resistance.** Real-time change in endothelial monolayer resistance was measured using the ECIS system (Applied Biophysics) to assess endothelial barrier function (Tiruppathi et al., 1992). In brief, after transfection, HMVEC-L were plated at confluence on a small gold electrode precoated with 0.2% gelatin. The small electrode and the larger counter electrode were connected to a phase-sensitive lock-in amplifier. An approximate constant current of 1 µA was supplied by a 1-V, 4,000-Hz alternating current signal connected serially to a 1-MΩ resistor between the small electrode and the larger counter electrode. The voltage between the small electrode and the large electrode was monitored by a lock-in amplifier, stored, and processed with a computer. The same computer controlled the output of the amplifier and switched the measurement to different electrodes in the course of an experiment. Before the experiment, the confluent endothelial monolayer was kept in 0.5% FBS-containing medium for 2 h. After 30–60 min of recording the TER at baseline, the endothelial monolayers were challenged with 4 U/ml of human α-thrombin (Enzyme Research Laboratories), and thrombin-induced change in resistance was monitored up to 13 h after the thrombin challenge.

**Imaging.** HMVEC-L were fixed with 4% paraformaldehyde and stained with anti–VE-cadherin (1:1,000; Sigma-Aldrich), or anti–β-catenin (1:200; Sigma-Aldrich). Nuclei were counterstained with DAPI. Cells were imaged with a confocal microscope system (LSM 510; Carl Zeiss, Inc.) equipped with a 63× 1.2 NA objective lens (Carl Zeiss, Inc.). The relative accumulation of β-catenin at AJs was quantified using 12-bit depth confocal z-series images. The maximum pixel values from different z sections were projected to the single plane using MetaMorph 7.1.0 software (MDS Analytical Technologies), and the integrated fluorescence intensity of threshold projected images was calculated for β-catenin. The values of the intensity threshold were selected using images of control untreated cells, and these values were retained for image analysis of samples from all experimental conditions. The integrated fluorescence intensities for β-catenin were plotted as median ± SD. The area of intercellular AJ gaps was quantified using MetaMorph 7.1.0 by manually outlining cells and selecting for gaps. The values are expressed as a percentage of the total surface area.

**Liposome-mediated gene transfer.** Liposomes were prepared as described previously (Bachmaier et al., 2007). In brief, the mixture, consisting of dimethyldioctadecylammonium bromide and cholesterol (1:1 molar ratio), was dried using the Rotavaporator (Brinkmann) and dissolved in

5% glucose followed by 20 min of sonication. The complex consisting of plasmid DNA (empty vector, or expressing β-catenin) and liposomes was combined at the ratio of 1 μg of DNA to 8 nmol of liposomes. The DNA–liposome complex (50 μg of DNA/mouse) was injected into the retro-orbital venous plexus.

**ChIP assay.** FoxM1-depleted or control HMVEC-L at 65 h after transfection were processed for a ChIP assay with a ChIP assay kit (Millipore) according to the manufacturer's instructions. In brief, HMVEC-L transfected with either FoxM1 siRNA or scRNA, or mock transfected, were cross-linked in situ by incubation with 1% formaldehyde at 37°C for 10 min, and sonicated (550 Sonic Dismembrator; Thermo Fisher Scientific) to generate DNA fragments at 500–1,000 bp. For the immunoprecipitation, 10 μg of anti-FoxM1 antibody (Santa Cruz Biotechnology) or control IgG were added to 300 μg of pre-cleared DNA sample and incubated overnight at 4°C with rotation. After serial washes, cross-links of DNA samples were reversed by incubation at 65°C for 4 h, and then isolated for quantitative real-time PCR analysis. PCR analysis was performed with a sequence detection system (ABI Prism 7000) using the following primers specific to the regulatory regions of the human *ctnnb1* gene: 5,739 bp upstream site, 5′-AAACTTTACAATTTGGCCATGAG-3′ and 5′-GGTAAGGACGTAGTCATTTCTG-3′; and 3,016 bp upstream site, 5′-AGCCAACCATGTAGTCTGACAAG-3′ and 5′-ACTTGGACTC-TACATCCGAATC-3′. DNA binding was normalized to control ChIP DNA samples immunoprecipitated with control rabbit serum.

**Statistical analysis.** The Student's *t* test and analysis of variance test were used to determine statistical significance. P-values $< 0.05$ denote the presence of a statistically significant difference.

**Online supplemental material.** Fig. S1 shows the absolute TER value, demonstrating impaired re-annealing of endothelial barrier in FoxM1-deficient HMVEC-L after the thrombin challenge. Fig. S2 demonstrates defective recovery of endothelial barrier in FoxM1-deficient EC monolayers after a challenge with histamine, which suggests that the defective AJ barrier recovery response was not mediator specific. Online supplemental material is available at http://www.jem.org/cgi/content/full/jem.20091857/DC1.

This work was supported by National Institutes of Health grant R01 HL085462 to Y.Y. Zhao. We thank Dr. Eric R. Fearon from the Department of Internal Medicine, University of Michigan Medical School, for his generosity in providing us the plasmid DNA expressing human β-catenin. We appreciate Drs. Yulia Komarova and Oleg Chaga from the Department of Pharmacology, University of Illinois at Chicago for their expert support with confocal microscopy imaging.

The authors have no conflicting financial interests.

**Submitted: 28 August 2009**
**Accepted: 16 June 2010**

## REFERENCES

Aberle, H., H. Schwartz, and R. Kemler. 1996. Cadherin-catenin complex: protein interactions and their implications for cadherin function. *J. Cell. Biochem.* 61:514–523. doi:10.1002/(SICI)1097-4644(19960616)61:4<514::AID-JCB4>3.0.CO;2-R

Aird, W.C. 2007. Phenotypic heterogeneity of the endothelium: I. Structure, function, and mechanisms. *Circ. Res.* 100:158–173. doi:10.1161/01.RES.0000255691.76142.4a

Bachmaier, K., S. Toya, X. Gao, T. Triantafillou, S. Garrean, G.Y. Park, R.S. Frey, S. Vogel, R. Minshall, J.W. Christman, et al. 2007. E3 ubiquitin ligase Cblb regulates the acute inflammatory response underlying lung injury. *Nat. Med.* 13:920–926. doi:10.1038/nm1607

Bazzoni, G., and E. Dejana. 2004. Endothelial cell-to-cell junctions: molecular organization and role in vascular homeostasis. *Physiol. Rev.* 84:869–901. doi:10.1152/physrev.00035.2003

Birukova, A.A., K. Smurova, K.G. Birukov, K. Kaibuchi, J.G. Garcia, and A.D. Verin. 2004. Role of Rho GTPases in thrombin-induced lung vascular endothelial cells barrier dysfunction. *Microvasc. Res.* 67:64–77. doi:10.1016/j.mvr.2003.09.007

Broman, M.T., P. Kouklis, X. Gao, R. Ramchandran, R.F. Neamu, R.D. Minshall, and A.B. Malik. 2006. Cdc42 regulates adherens junction stability and endothelial permeability by inducing alpha-catenin interaction with the vascular endothelial cadherin complex. *Circ. Res.* 98:73–80. doi:10.1161/01.RES.0000198387.44395.e9

Camerer, E., I. Cornelissen, H. Kataoka, D.N. Duong, Y.W. Zheng, and S.R. Coughlin. 2006. Roles of protease-activated receptors in a mouse model of endotoxemia. *Blood.* 107:3912–3921. doi:10.1182/blood-2005-08-3130

Carmeliet, P., M.G. Lampugnani, L. Moons, F. Breviario, V. Compernolle, F. Bono, G. Balconi, R. Spagnuolo, B. Oosthuyse, M. Dewerchin, et al. 1999. Targeted deficiency or cytosolic truncation of the VE-cadherin gene in mice impairs VEGF-mediated endothelial survival and angiogenesis. *Cell.* 98:147–157. doi:10.1016/S0092-8674(00)81010-7

Cattelino, A., S. Liebner, R. Gallini, A. Zanetti, G. Balconi, A. Corsi, P. Bianco, H. Wolburg, R. Moore, B. Oreda, et al. 2003. The conditional inactivation of the β-catenin gene in endothelial cells causes a defective vascular pattern and increased vascular fragility. *J. Cell Biol.* 162:1111–1122. doi:10.1083/jcb.200212157

Clark, K.L., E.D. Halay, E. Lai, and S.K. Burley. 1993. Co-crystal structure of the HNF-3/fork head DNA-recognition motif resembles histone H5. *Nature.* 364:412–420. doi:10.1038/364412a0

Costa, R.H. 2005. FoxM1 dances with mitosis. *Nat. Cell Biol.* 7:108–110. doi:10.1038/ncb0205-108

Coughlin, S.R. 2000. Thrombin signalling and protease-activated receptors. *Nature.* 407:258–264. doi:10.1038/35025229

Dejana, E. 2004. Endothelial cell-cell junctions: happy together. *Nat. Rev. Mol. Cell Biol.* 5:261–270. doi:10.1038/nrm1357

Dejana, E., F. Orsenigo, and M.G. Lampugnani. 2008. The role of adherens junctions and VE-cadherin in the control of vascular permeability. *J. Cell Sci.* 121:2115–2122. doi:10.1242/jcs.017897

Huber, A.H., D.B. Stewart, D.V. Laurents, W.J. Nelson, and W.I. Weis. 2001. The cadherin cytoplasmic domain is unstructured in the absence of beta-catenin. A possible mechanism for regulating cadherin turnover. *J. Biol. Chem.* 276:12301–12309. doi:10.1074/jbc.M010377200

Huelsken, J., R. Vogel, V. Brinkmann, B. Erdmann, C. Birchmeier, and W. Birchmeier. 2000. Requirement for β-catenin in anterior-posterior axis formation in mice. *J. Cell Biol.* 148:567–578. doi:10.1083/jcb.148.3.567

Kaestner, K.H., W. Knochel, and D.E. Martinez. 2000. Unified nomenclature for the winged helix/forkhead transcription factors. *Genes Dev.* 14:142–146.

Kalinichenko, V.V., M.L. Major, X. Wang, V. Petrovic, J. Kuechle, H.M. Yoder, M.B. Dennewitz, B. Shin, A. Datta, P. Raychaudhuri, and R.H. Costa. 2004. Foxm1b transcription factor is essential for development of hepatocellular carcinomas and is negatively regulated by the p19ARF tumor suppressor. *Genes Dev.* 18:830–850. doi:10.1101/gad.1200704

Korver, W., M.W. Schilham, P. Moerer, M.J. van den Hoff, K. Dam, W.H. Lamers, R.H. Medema, and H. Clevers. 1998. Uncoupling of S phase and mitosis in cardiomyocytes and hepatocytes lacking the winged-helix transcription factor Trident. *Curr. Biol.* 8:1327–1330. doi:10.1016/S0960-9822(07)00563-5

Krupczak-Hollis, K., X. Wang, V.V. Kalinichenko, G.A. Gusarova, I.C. Wang, M.B. Dennewitz, H.M. Yoder, H. Kiyokawa, K.H. Kaestner, and R.H. Costa. 2004. The mouse Forkhead Box m1 transcription factor is essential for hepatoblast mitosis and development of intrahepatic bile ducts and vessels during liver morphogenesis. *Dev. Biol.* 276:74–88. doi:10.1016/j.ydbio.2004.08.022

Lampugnani, M.G., and E. Dejana. 2007. Adherens junctions in endothelial cells regulate vessel maintenance and angiogenesis. *Thromb. Res.* 120:S1–S6. doi:10.1016/S0049-3848(07)70124-X

Lampugnani, M.G., M. Corada, L. Caveda, F. Breviario, O. Ayalon, B. Geiger, and E. Dejana. 1995. The molecular organization of endothelial cell to cell junctions: differential association of plakoglobin, β-catenin, and α-catenin with vascular endothelial cadherin (VE-cadherin). *J. Cell Biol.* 129:203–217. doi:10.1083/jcb.129.1.203

Laoukili, J., M.R. Kooistra, A. Brás, J. Kauw, R.M. Kerkhoven, A. Morrison, H. Clevers, and R.H. Medema. 2005. FoxM1 is required for execution of the mitotic programme and chromosome stability. *Nat. Cell Biol.* 7:126–136. doi:10.1038/ncb1217

Mehta, D., and A.B. Malik. 2006. Signaling mechanisms regulating endothelial permeability. *Physiol. Rev.* 86:279–367. doi:10.1152/physrev.00012.2005

Navarro, P., L. Caveda, F. Breviario, I. Mândoteanu, M.G. Lampugnani, and E. Dejana. 1995. Catenin-dependent and -independent functions of vascular endothelial cadherin. *J. Biol. Chem.* 270:30965–30972. doi:10.1074/jbc.270.52.30965

Tauseef, M., V. Kini, N. Knezevic, M. Brannan, R. Ramchandaran, H. Fyrst, J. Saba, S.M. Vogel, A.B. Malik, and D. Mehta. 2008. Activation of sphingosine kinase-1 reverses the increase in lung vascular permeability through sphingosine-1-phosphate receptor signaling in endothelial cells. *Circ. Res.* 103:1164–1172. doi:10.1161/01.RES.0000338501.84810.51

Tiruppathi, C., A.B. Malik, P.J. Del Vecchio, C.R. Keese, and I. Giaever. 1992. Electrical method for detection of endothelial cell shape change in real time: assessment of endothelial barrier function. *Proc. Natl. Acad. Sci. USA.* 89:7919–7923. doi:10.1073/pnas.89.17.7919

Tiruppathi, C., M. Freichel, S.M. Vogel, B.C. Paria, D. Mehta, V. Flockerzi, and A.B. Malik. 2002. Impairment of store-operated Ca2+ entry in TRPC4(-/-) mice interferes with increase in lung microvascular permeability. *Circ. Res.* 91:70–76. doi:10.1161/01.RES.0000023391.40106.A8

Vogel, S.M., X. Gao, D. Mehta, R.D. Ye, T.A. John, P. Andrade-Gordon, C. Tiruppathi, and A.B. Malik. 2000. Abrogation of thrombin-induced increase in pulmonary microvascular permeability in PAR-1 knockout mice. *Physiol. Genomics.* 4:137–145.

Wang, I.C., Y.J. Chen, D. Hughes, V. Petrovic, M.L. Major, H.J. Park, Y. Tan, T. Ackerson, and R.H. Costa. 2005. Forkhead box M1 regulates the transcriptional network of genes essential for mitotic progression and genes encoding the SCF (Skp2-Cks1) ubiquitin ligase. *Mol. Cell. Biol.* 25:10875–10894. doi:10.1128/MCB.25.24.10875-10894.2005

Ware, L.B., and M.A. Matthay. 2000. The acute respiratory distress syndrome. *N. Engl. J. Med.* 342:1334–1349. doi:10.1056/NEJM200005043421806

Weis, S.M., and D.A. Cheresh. 2005. Pathophysiological consequences of VEGF-induced vascular permeability. *Nature.* 437:497–504. doi:10.1038/nature03987

Wierstra, I., and J. Alves. 2007. FOXM1, a typical proliferation-associated transcription factor. *Biol. Chem.* 388:1257–1274. doi:10.1515/BC.2007.159

Zhao, Y.Y., X.P. Gao, Y.D. Zhao, M.K. Mirza, R.S. Frey, V.V. Kalinichenko, I.C. Wang, R.H. Costa, and A.B. Malik. 2006. Endothelial cell-restricted disruption of FoxM1 impairs endothelial repair following LPS-induced vascular injury. *J. Clin. Invest.* 116:2333–2343. doi:10.1172/JCI27154

Zhao, Y.D., H. Ohkawara, S.M. Vogel, A.B. Malik, and Y.Y. Zhao. 2010. Bone marrow-derived progenitor cells prevent thrombin-induced increase in lung vascular permeability. *Am. J. Physiol. Lung Cell. Mol. Physiol.* 298:L36–L44. doi:10.1152/ajplung.00064.2009